POLYETHERSULFONE COMPOSITE MEMBRANE BLENDED WITH CELLULOSE FIBRILS

Ping Qu,[a] Huanwei Tang,[a] Yuan Gao,[a] Li-ping Zhang,[a] * and Siqun Wang [b]

Polyethersulfone (PES) is a common material used for ultrafiltration (UF) membranes, which has good chemical resistance, high mechanical properties, and wide temperature tolerances. The hydrophobic property of the PES membrane seriously limits its application. Cellulose fibrils are composed of micro-sized and nano-sized elements, which have high hydrophilicity, strength, and biodegradation. A composite membrane was prepared by the phase inversion induced by an immersion process. The characteristics of the composite membrane were investigated with Fourier transform infrared spectroscopy (FTIR), X-ray diffraction (XRD), thermogravimetric analysis (TGA), and atomic force microscopy (AFM). The pure water flux of the composite membrane increased dramatically with the increase of cellulose firbils. Mean pore size and porosity were significantly increased. Both mechanical properties and hydrophilicity were enhanced due to the addition of the cellulose firbils.

Keywords: Poly(ether sulfones); Cellulose fibrils; Membranes; Hydrophilic property

*Contact information: a: College of Material Science and Technology, Beijing Forestry University, Beijing, 100083, PR China; b: Tennessee Forest Products Center, University of Tennessee, 2506 Jacob Dr., Knoxville, TN37996-4570, USA; * Corresponding author: zhanglp418@163.com*

INTRODUCTION

Ultrafiltration (UF) membranes have been widely applied in modern industry, including applications in water treatment, the foodstuffs industry, and pharmaceuticals (Kim et al. 1999). Polyethersulfone (PES) is extensively used as one of the membrane materials. It has favorable characteristics of good chemical resistance, high strength, wide temperature tolerances, and high dimensional stability to be fabricated into membranes in various conditions for UF (Li et al. 2008). Phase inversion with immersion, simply operated, is one of the most common methods to prepare asymmetric polymeric membranes (Madaeni and Rahimpour 2005; Rahimpour et al. 2007). Permeability and selectivity are controlled by the surface layer of the membrane. However, in water treatment, pure PES membrane is vulnerable to fouling due to the hydrophobic character of PES material (Khulbe et al. 2007; Kim et al. 1999). Severe problems can be caused by protein, which can easily form a layer on a PES membrane surface under hydrophobic conditions during the operation (Khulbe et al. 2000; Ho and Zydney 1999; Lindau and Jönsson 1999). Eventually, membrane fouling results in not only limiting of UF membrane performance and reducing its working life, but also in increasing the operating cost. Hydrophobicity seriously limits the application of PES membranes. However, the hydrophilic character of membranes can be improved by blending with hydrophilic materials. Blending is known to be a very effective method of producing membrane

materials with improvement of membrane properties. Some inorganic particles, such as TiO_2 and SiO_2, have been used to enhance the mechanical properties of membranes (Arthanareeswaran et al. 2008; Devrim et al. 2009; Yu et al. 2009). However, the most significant problem in blending process is how to disperse particles into the polymer casting solution uniformly.

Cellulose is the most abundant natural biopolymer found in the world, and it has considerable advantages, such as environmental friendliness, biodegradability, and renewability (Li et al. 2009; Goetz et al. 2009; Zuluaga et al. 2009). One significant hot issue is the development of cellulose fibrils. Cellulose fibrils can be prepared in the nano and micro scales (Cheng et al. 2009). Currently, cellulose fibrils can be produced by mechanical or chemical treatment. The chemical method, for instance by using strong acid hydrolysis (Li et al. 2009; Beck-Candanedo et al. 2005), generates size-controlled fibrils with partial removal of the amorphous regions of wood fibers, cotton, and parts of sea animals that are used as raw materials (Hubbe et al. 2008; Beck-Candanedo et al. 2005; Morán et al. 2008). The mechanical method can include a grinder treatment, a high-pressure homogenizer treatment, and a high-pressure refiner treatment (Abe et al. 2007; Chakraborty et al. 2005; Herrick et al. 1983). Cellulose fibrils generated from cellulose pulp have much larger specific surface area and higher stiffness than others (Lee et al. 2009). Compared with the inorganic particles, cellulose fibrils with a high axis ratio (L/d) have received significant attention due to their low density and their biocompatibility, as well as easy availability and renewability (Lu et al. 2008; Li et al. 2009). In addition, the better hydrophilic property of cellulose fibrils compared to many other fibrous materials is ascribed to abundant exposed hydroxyl (-OH) groups (Andresen et al. 2006; Lu et al. 2008; Nishino et al. 1995). Generally, cellulose fibrils are very attractive for reinforcing polymers and for enhancing the hydrophilic character when preparing composite materials (Ganster and Fink 2006).

In order to improve the hydrophilicity of PES membranes, some hydrophilic cellulose fibrils could be blended with PES. In our previous study, cellulose fibrils were uniformly dispersed into PES casting solution by ultrasonic treatment to prevent their agglomeration. The UF properties of composite membrane were evaluated directly by an ultrafiltration process. An obtained composite membrane was characterized by Fourier transform infra-red spectrometry (FT-IR), X-ray diffraction (XRD), and thermogravimetric analysis (TGA). The mechanical properties and morphologies of pure PES membrane and composite membrane were measured and compared by tensile tests and observations of atomic force microscopy (AFM), respectively.

EXPERIMENTAL

Materials

Cellulose fibrils in micro and nano scales were prepared according to Qu et al. (2010). Polyethersulfone (PES, Mw=140,000, purchased from Beijing Trihigh membrane co., Beijing, China) was used as the polymer. Polyvinylpyrrolidone (PVP) (K30, CP, importation) and N,N-Dimethylacetamide (DMAC) were purchased from Beijing Chemical Reagent Company and Beijing Chemical Plant (Beijing, China), respectively.

Bovine Serum Albumin (BSA) (BR) was purchased from Beijing Aoboxing Biological Technology Limited Company (Beijing, China).

Preparation of Composite Membrane

The Loeb and Sorirajan phase inversion method was used to prepare the composite membrane. Some cellulose fibrils (in different contents) were dispersed in the DMAC by ultrasonic treatment for 30 min at 30 °C and 100 Hz (numerical control ultrasonic cleaner, KQ5200DB, Zhengzhou, China). Then PES (18 wt %) and PVP K30 (0.3 wt %) were added into the above solution. After being swayed in the table concentrator at 30 °C and 120 r/min for 48 h (constant temperature table concentrator, SHK-99-II, Beijing, China), the casting solution was obtained. The casting solution was treated with vacuum to get rid of gas at a vacuum degree of -0.1 MPa, and then the above solution was scraped to a thin layer by a scraper on the glass board. After being vaporized in the air for 10 s, the thin layer was immersed into a coagulation bath (water) to form the composite membrane. Before being tested, the prepared membrane was dipped in distilled water for 24 h. The thickness of membrane was about 200 μm.

Table 1. Formulations of Prepared Solution

Sample	Cellulose fibrils (wt %)	PES (wt %)	PVP K30 (wt %)
1	0	18	0.3
2	0.2	18	0.3
3	0.5	18	0.3
4	1	18	0.3
5	1.5	18	0.3
6	2	18	0.3
7	2.5	18	0.3
8	3	18	0.3
9	4	18	0.3

Membrane Hydrophilicity

The contact angles θ can be used to measure the degree of hydrophilicity. The contact angles between water and composite membranes with different contents of cellulose fibrils were measured by a contact angle goniometer (JGW-360a, Hebei, China). The surface energy W_A can be calculated by following equation (5),

$$W_A = \gamma_W \cdot (1+\cos\theta) \quad (5)$$

where the surface tension γ_W is 7.28×10^{-2} N/m.

Fourier Transform Infrared Spectroscopy (FT-IR)

The membranes, cut to pieces as small as possible, were blended with potassium bromide (KBr). The mixtures were ground to powders and then pressed into transparent flakes. The flakes were measured with FTIR (Tensor 27, Bruker, Germany).

Atomic Force Microscope (AFM)

The morphologies of pure PES membrane and composite membrane were observed using an atomic force microscope (SHIMADZU SPn9000, Japan) with non-contact mode after they were dried on a silicon wafer. The images of surface layer and porous support layer were analyzed. The roughness data (R_q) of the composite membrane surfaces and the compared were calculated by SPM offline software.

Ultrafiltration Properties of Composite Membrane

The pure water flux and rejection were measured by an ultrafiltration process (see Fig. 1). The tests were operated under a working pressure of 0.1 MPa and at room temperature.

Fig. 1. Apparatus for evaluation of ultrafiltration characteristics: 1 - Connection of the steel bottle to a source of N_2 to maintain the pressure; 2 - Feeding hole; 3 - Rotor; 4 - Discharging hole; 5 - Ultrafiltration membrane

The following procedure was used to measure the ultrafiltration properties of composite membranes by means of the device shown in Fig. 1. After installation of the ultrafiltration membrane, pure water or BSA solution was poured into the device through the feeding hole. The rotor was set into motion, and the steel bottle was connected to the N_2 supply to maintain a pressure of 0.1 MPa, after which the test began. The pure water flux [J_w ($L \cdot m^{-2} \cdot h^{-1}$)] was calculated with the following equation,

$$J_w = V/(At) \quad (1)$$

where V is the volume of filtered water (m^3), A is the membrane area (m^2), and t is the working time (h).

The rejection was tested by filtrating BSA solution (1 g/L), and the absorbencies of raw BSA solution and filtrated solution were measured at 280 nm with ultraviolet visible spectrophotometer UV-9100(Shanghai, China). Then the rejection was calculated using equation (2),

$$R = (1\text{-}A_p/A_b) \times 100\% \quad (2)$$

where R is the rejection ratio (%) and A_p and A_b are the absorbances of the filtered and raw solutions, respectively.

The membrane, having a known area, was weighed in the wet state and then dried in an oven. The porosity [P_r (%)] and mean pore size [r (m)] of the membrane were evaluated using equations (3) and (4),

$$P_r = (W_w - W_d)/(d_w A_m L_m) \quad (3)$$

where W_w is the weight of the wet membrane (g); W_d is the weight of the dry membrane (g); d_w is the water density (g/cm^3); and A_m and L_m are the membrane area (cm^2) and thickness (cm), respectively, and,

$$r = [8 \times (2.9\text{-}1.75P_r) \cdot \eta LF/3600P_r\Delta P]^{1/2} \quad (4)$$

where η is the viscosity of water (Pa·s), L is the membrane thickness (m), F is the pure water flux (m^3/m^2·h), and ΔP is the working pressure (Pa). Equations 1 through 4 were calculated according to Zhang et al. (2009).

Tensile Strength and Elongation

The mechanical properties were tested by a tensile testing machine (DCP-KZ300, Sichuan, China). The cross head speed was 20 mm/min. The samples were cut into pieces in a rectangular shape with width of 15mm and total length of 100 mm, and then dried at 100 °C.

Crystallinity

The crystallinities of cellulose fibrils and composite membrane were tested with an X-ray diffraction instrument (Shimadzu XRD-6000, Japan) with Cu, Kcr radial, Ni filter, X=0.154 nm, scan range: 2θ= 5-40°, and scan step: =0.2°/3 s. Then the crystallinities were calculated.

Thermogravimetric Properties (TGA)

The thermogravimetric behavior was characterized by a thermogravimetric analysis instrument (Shimadzu TGA-600, Japan). The temperature range was from 30 °C to 600 °C with a heating rate of 10 °C/min. The test was carried out under nitrogen atmosphere (20 ml/min) in order to prevent thermoxidative degradations.

RESULTS AND DISCUSSION

Hydrophilic Properties of Composite Membrane

The hydrophilicity of a polymer material can be evaulated by its contact angle (θ) with water. In general, membrane surface hydrophilicity is higher when its contact angle is smaller. Contact angle and surface energy of the pure PES membrane and composite membranes with different contents of cellulose fibrils are shown in Fig. 2. Compared to the pure PES membrane, the contact angles of the composite membranes dropped gradually from 55.8 º to 45.8 º, and surface energies were increased from 113.7 mN/m^2 to 123.5 mN/m^2 with increasing cellulose content. This result implies that hydrophilic

cellulose fibrils, which contained hydroxyl groups, were exposed on the membrane surface.

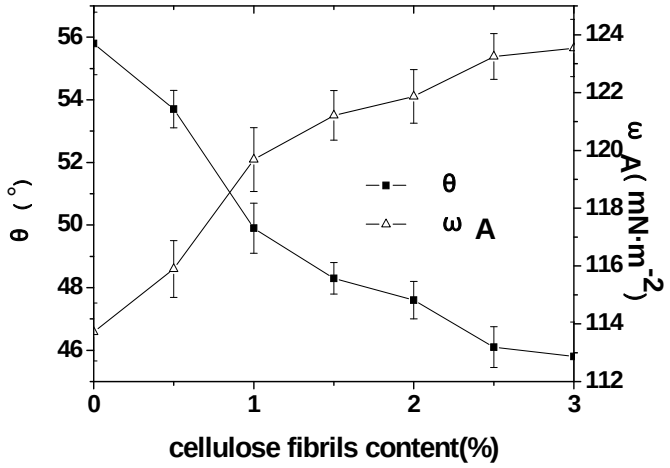

Figure 2. Effect on hydrophilic angle (a) and surface energy(b) of composite memebrane with different cellulose fibrils contents

Infrared Spectroscopy Analysis

Specific absorption peaks can be identified for particular groups in FTIR. Figure 3 shows the spectra of cellulose fibrils (a), pure PES membrane (b), and composite membrane (c). From spectrum a, it was observed that the hydrogen bond O-H stretching at 3347 cm^{-1}, the C-H stretching at 2903 cm^{-1}, the -CH_2 bending at 1429 cm^{-1}, and the C-H bending at 1370 cm^{-1} represented characteristic peaks of cellulose. The peak at 1058 cm^{-1} was related to the CO stretching. The CH bending and CH_2 stretching at 899 cm^{-1} indicated the amorphous structure of cellulose fibrils. In addition, the peak at 1635 cm^{-1} was detected as the O-H bending of adsorbed water, because water adsorbed in the cellulose molecules was too difficult to extract. Spectrum b shows characteristic peaks of PES molecular structure. The PES structure includes a benzene ring, an ether bond, and a sulphone structure. The C-H stretching peak of benzene ring was situated at 3097 cm^{-1}. Three peaks between 1600 cm^{-1} and 1400 cm^{-1} were attributed to aromatic skeletal vibration. The C-O-C stretching peaks were located at 1324 cm^{-1} and 1239 cm^{-1}. The S=O stretching peaks were present at 1151 cm^{-1} and 1105 cm^{-1}.

From spectra a and c, the OH stretching peak became apparently wide and strong in the 3200 cm^{-1}- 3700 cm^{-1} region. This indicated that hydrogen bonds were formed between OH groups of cellulose molecular and oxygen atom in ether and sulphone groups of PES. And characteristic peaks of cellulose fibrils were present in the spectrum c. It was the evidence that cellulose fibrils were kept in the composite membrane. However, C-O-C and C-O stretching peaks were not observed, since they might be covered by other strong peaks of PES absorption bands. Upon comparison of spectra b and c, characteristic peaks of pure PES membrane were displayed in spectrum c. For instance, benzene ring skeletal vibration peaks were displayed at 1579 cm^{-1}, 1475 cm^{-1}, and 1411 cm^{-1}. The C-O-C and S=O stretching peaks were present at their original locations. No new peaks appeared in the spectra of composite membrane. This could be

explained as evidence that cellulose fibrils and PES did not produce new function groups during the preparation of composite membrane. Also cellulose and PES were interacting together at a molecular level. The wave numbers of absorption bands in composite membrane fluctuated to some extent.

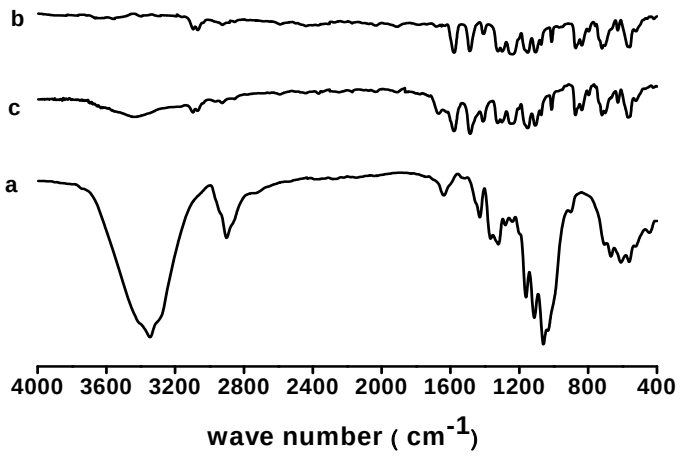

Figure 3. FTIR of cellulose fibrils (a), pure PES membrane (b) and composite membrane (c)

Morphology of Composite Membrane

Two-dimensional surface layer images and three-dimensional porous support layer images of the pure PES membrane and composite membrane are given in Figs. 4 and 5, which show the overall morphology of membrane materials. In these images, the dimensions of surface layer and porous support layer are 1μm ×1μm and 5μm ×5μm, respectively. In addition, the color brightness represents the vertical dimension of the membrane. The convex areas are displayed as light areas and the membrane pores are shown as dark spots. The surface layers of the pure PES membrane and composite membrane were rough. The roughness data (R_q) of the composite membrane surfaces and the compared were 41.76 nm and 77.21 nm, respectively. Dense membrane structures were apparent, and the surface of the each membrane was rough and uneven. The porous support layers of both the pure PES membrane and the composite membrane showed loose membrane structures. However, the mean pore size of the composite membrane was larger than that of the pure PES membrane. Compared with the pure PES membrane, the pores were well distributed in the composite membrane. An asymmetric membrane structure was observed from the surface layer and the porous support layer by the AFM images.

Effects of Cellulose Fibrils on Ultrafiltration Performance

Figure 6 shows pure water flux and BSA rejection results for the pure PES membrane and composite membranes with different contents of cellulose fibrils. The operating pressure and temperature were 0.1 MPa and 25 °C, respectively. The pure water flux of composite membrane increased with increasing the content of cellulose fibrils and then decreased. At the same time, BSA rejections of composite membranes remained at a higher level, 91% to 95%.

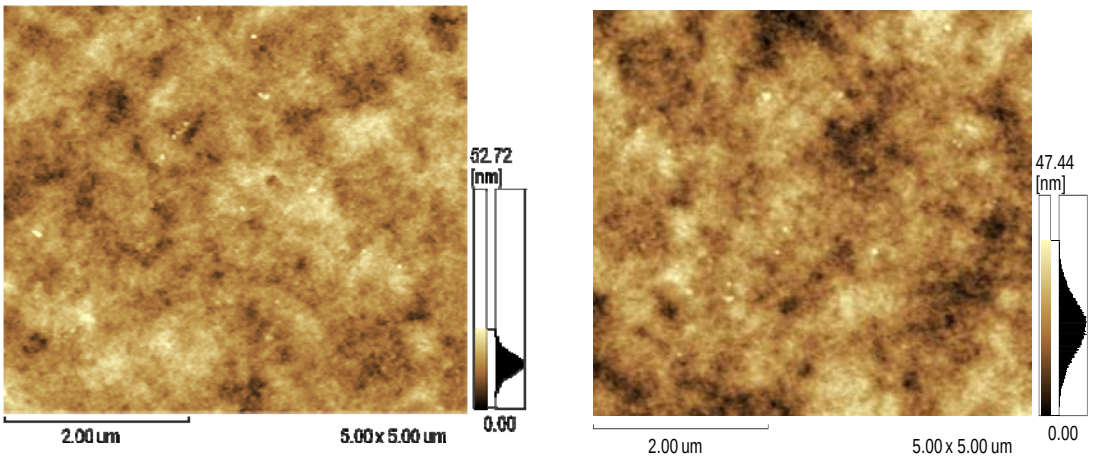

(a) (b)

Figure 4. AFM images of pure PES membrane (a) and composite membrane (b) surface layer

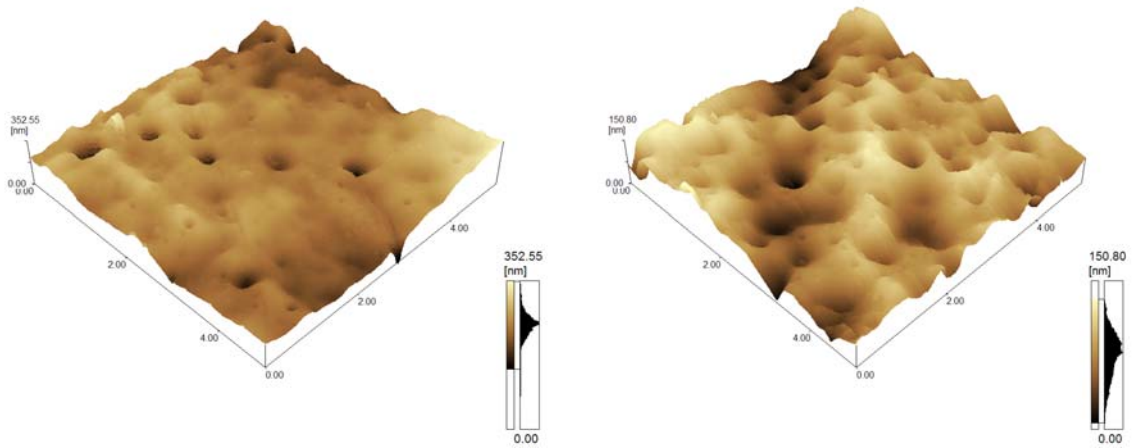

(a) (b)

Figure 5. AFM images of pure PES membrane (a) and composite membrane (b) support layer

The pure water flux (PWF) of composite membrane reached a maximum value of 813.3 $L \cdot m^{-2} \cdot h^{-1}$ when the content of cellulose fibrils was 1 wt % of the casting solution. This flux increased by 1.36 times compared to that of pure PES membrane. The difference could be attributed to the fact that the instantaneous phase separation process was accelerated because of cellulose fibrils during the preparation of composite membrane. Consequently, the composite membrane had higher porosity, larger pore size, and better connectivity. In addition, the hydrophilic nature of the composite membrane could be effectively enhanced by cellulose fibrils, exposing a great amount of hydroxyl groups in the surface. As is expected, the pure water flux of composite membrane was increased significantly. However, at sufficiently high addition levels cellulose fibrils in the composite membrane might block membrane pores significantly, resulting in the slight decrease of pure water flux of composite membrane when the content of cellulose fibrils was more than 1 wt %.

Figure 7 reveals the effects of the content of cellulose fibrils on porosity and mean pore size. The porosity and mean pore size first increased and then decreased, with a maximum value of porosity 88.8 % when the content of cellulose fibrils was 1 wt % of the casting solution, and a peak value of mean pore size 70.9 nm when the content of cellulose firbils was 1 wt %. In comparison with pure PES membrane, the porosity and mean pore size of the composite membrane improved 39.1 % and 30.6 %, respectively. This change could be attributed to the fact that cellulose fibrils were better dispersed in PES casting solution, which relatively decreased the content of organic solvent, DMAC. The components of the casting solution were changed owing to the existence of cellulose fibrils at the phase separation process. In addition, the multi-exchange rate between DMAC and water was accelerated by the strong hydrophilicity of cellulose fibrils. Also the high multi-exchange rate facilitated phase separation and growth of a polymer-poor phase. These processes were beneficial for the formation of a composite membrane with higher porosity and larger mean pore size. However, cellulose fibrils might also have blocked pores of the composite membrane to a significant extent when the content of cellulose fibrils was more than 1 %.

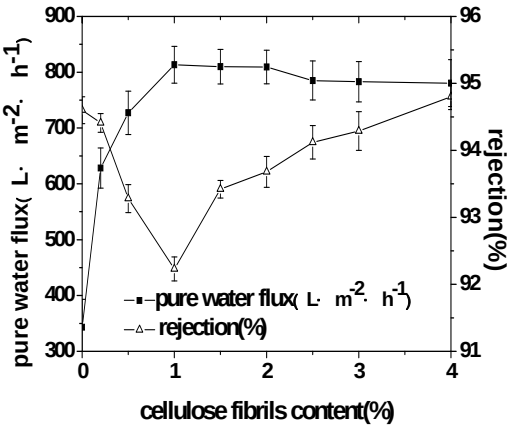

Figure 6. Effect on pure water flux and rejection of composite membrane with different cellulose fibrils contents

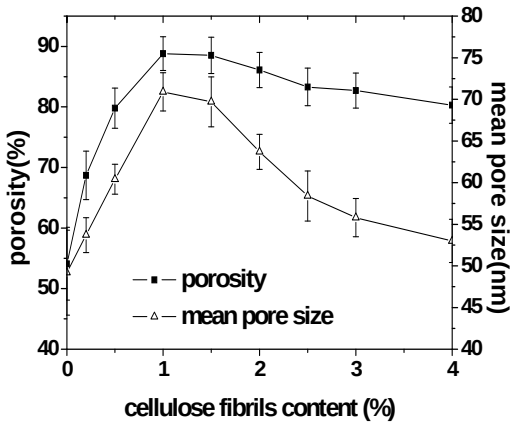

Figure 7. Effect content on porosity (a) and mean pore size (b) of the composite membrane with different cellulose fibrils contents

Mechanical Properties of Composite Membrane

Figure 8 displays the effect of the content of cellulose fibrils on mechanical properties of the composite membrane. The tensile strength of composite membrane was 7.25 MPa and elongation was 11.6 %, when the optimal content of cellulose fibrils was 1 wt % of the casting solution. The results demonstrated that mechanical properties of composite membrane were enhanced with the addition of cellulose fibrils. The cellulose fibrils exposed considerable surface hydroxyl groups and possessed high reaction activity. The interface combination was formed by the cross-link network of hydrogen bonds between PES and cellulose fibrils. However, cellulose fibrils easily aggregated and dispersed nonuniformly in the polymer matrix when the amount of cellulose fibrils added was larger. As a result, the mechanical stability of the composite membrane was

weakened. The polyethersulfone composite membrane blended with appropriate amount of cellulose fibrils improved the membrane's mechanical properties.

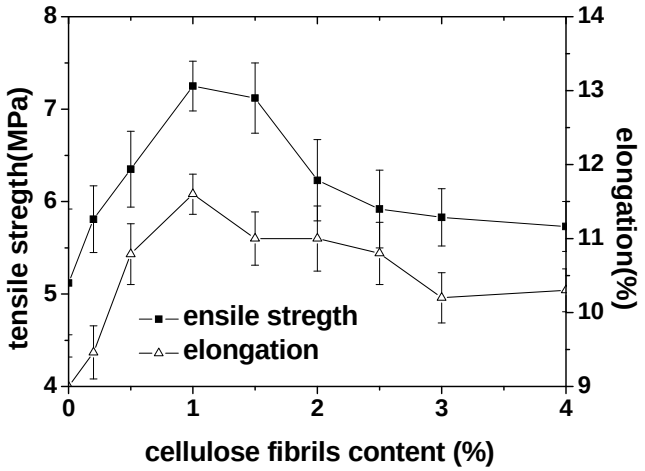

Figure 8. Effect on tensile strength and elongation of the composite membrane with different cellulose fibrils contents

XRD of Composite Membrane

Figure 9 displays the typical X-ray diffraction of cellulose fibrils. It shows two peaks, both of which indicated that the cellulose fibrils were semi-crystalline, containing crystalline regions and amorphous regions. The two peaks were situated at 2θ = 16.6 ° and 2θ = 22.6 °, which represented (002) and (001) crystallographic planes, respectively. Both of the two peaks could be attributed to cellulose I, which has a monoclinic structure. Estimation of the crystallinity index was 64.9 %. Figure 10 shows diffractograms of pure PES membrane and composite membrane. The larger rigid benzene ring and the more flexible ether bond structure together form amorphous PES. Figure 10 shows the XRD pattern for the pure PES and composites membrane. It is possible to see peaks at 2θ = 16.6° and 2θ = 22.6°, indicating cellulose I structure. This imples that the cellulose structure was retained after the compounding process (Oksman et al. 2006).

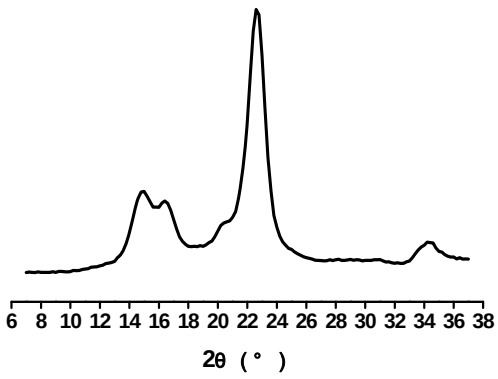

Figure 9. X - ray diffraction of cellulose fibrils

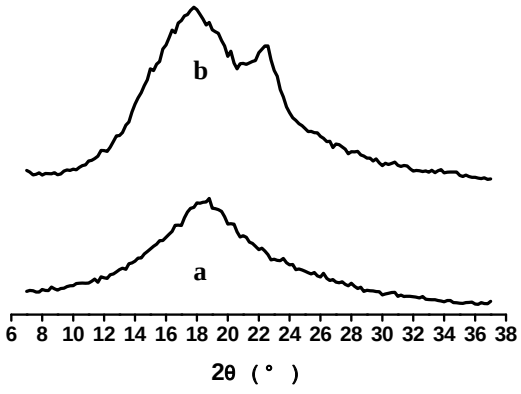

Figure 10. X - ray diffraction of pure PES membrane (a) and composite membrane (b)

TGA of Composite Membrane

The thermogravimetric curves of cellulose fibrils, pure PES membrane, and composite membrane are presented in Figure 11. Cellulose fibrils and PES usually decompose at different temperatures, due to the differences in the chemical structures. In curve a, the weight loss started at 285 ºC and persisted until 380 ºC, showing a solid residual at 600 ºC. This stage was attributed to the decomposition of cellulose fibrils. From curve b, the decomposition temperature of pure PES membrane was about 500 ºC, with weight losing stage from 500 ºC to 600 ºC. From curve c, there existed two decomposition stages in the ranges of 320 ºC to 400 ºC and 500 ºC to 600 ºC. The stages indicated that cellulose fibrils were decomposed first. Then the second one in the range of 500 ºC to 600 ºC, represented a weight loss process of PES. Compared to curves a and c, the decomposition temperature of cellulose fibrils in the composite membrane was higher than that of pure cellulose fibrils materials. These results demonstrated that there were interactions between cellulose fibrils and PES materials. From the molecular structural characteristics, hydrogen bonds could be formed between hydroxyl groups of cellulose fibrils and function groups of PES, which resulted in a higher decomposition temperature of cellulose fibrils in the composite membrane. The thermogravimetric curve of the composite membrane did not show obvious weight loss until the temperature reached 300 ºC. This indicates that composite membrane materials could fully satisfy the demands of various membrane applications.

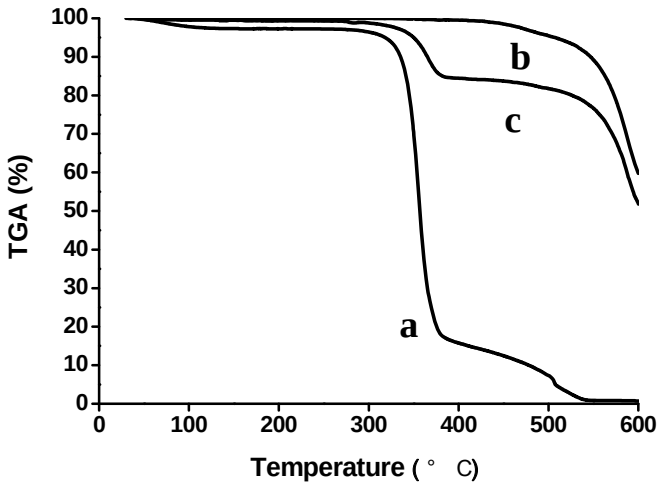

Figure 11. TGA curves of cellulose fibrils (a), pure PES membrane (b) and composite membrane (c)

CONCLUSIONS

1. A composite membrane of polyethersulfone blended with cellulose fibrils by ultrasonic treatment, was prepared by the L-S phase inversion process. The contact angle decreased and surface energy increased with increasing content of cellulose fibrils. FT-IR analysis showed that a suitable level of molecular compatibility was

achieved, which was based on the existence of inter-molecular hydrogen bonds between PES and cellulose fibrils. The surface layer of the composite membrane material was dense, and the support layer of the composite membrane had larger size pores than that of a pure PES membrane. The cellulose fibrils changed both properties and structures of the composite membrane.

2. The pure water flux of composite membrane increased with increasing the content of cellulose fibrils and then decreased. At the same time, BSA rejections of composite membranes remained at a higher level. The pure water flux of composite membrane reached a maximum value of 813.3 $L \cdot m^{-2} \cdot h^{-1}$ when the content of cellulose fibrils was 1 wt % of the casting solution. At the same content of cellulose fibrils, the porosity and mean pore size of composite membrane were 88.8 % and 70.9 nm, respectively. In comparison with pure PES membrane, the porosity and mean pore size of composite membrane was improved by 39.1 % and 30.6 %
3. Both tensile strength and elongation of composite membrane were improved in comparation with mechanical properties of pure PES membrane. XRD results showed that the cellulose structure in composite membranes was retained after the compounding process. A higher decomposition temperature of cellulose fibrils in the composite membrane demonstrated that there were interactions between cellulose fibrils and PES materials. Two weight loss stages existed in the TGA curves of composite membrane because of thermal degradation of PES and cellulose fibrils, respectively.

ACKNOWLEDGMENTS

The authors are thankful for the financial support of the Major State Basic Research Development Program of China (973 Program) (No. 2010CB732204) and China Ministry of Education (B08005) and State Forestry Administration (2008-4-075).

REFERENCES CITED

Abe, K., Iwamoto, S., and Yano, H. (2007). "Obtaining cellulose nanofibers with a uniform width of 15 nm from wood." *Biomacromolecules* 8(10), 3276-3278.

Andresen, M., Johansson, L., Tanem, B., and Stenius, P. (2006). "Properties and characterization of hydrophobized microfibrillated cellulose," *Cellulose* 13(6), 665-677.

Arthanareeswaran, G., Sriyamuna Devi, T. K., and Raajenthiren, M. (2008). "Effect of silica particles on cellulose acetate blend ultrafiltration membranes: Part I," *Separation and Purification Technology* 64(1), 38-47.

Beck-Candanedo, S., Roman, M., and Gray, D. G. (2005). "Effect of reaction conditions on the properties and behavior of wood cellulose nanocrystal suspensions," *Biomacromolecules* 6(2), 1048-1054.

Chakraborty, A., Sain, M., and Kortschot, M. (2005). "Cellulose microfibrils: A novel method of preparation using high shear refining and cryocrushing," *Holzforschung*,

59(1), 102-107.
Cheng, Q., Wang, S., and Rials, T. G. (2009). "Poly (vinyl alcohol) nanocomposites reinforced with cellulose fibrils isolated by high intensity ultrasonication," *Composites Part A: Applied Science and Manufacturing* 40(2), 218-224.
Devrim, Y., Erkan, S., Ba, N., and Eroglu, I. (2009). "Preparation and characterization of sulfonated polysulfone/titanium dioxide composite membranes for proton exchange membrane fuel cells," *International Journal of Hydrogen Energy* 34(8), 3467-3475.
Ganster, J., and Fink, H. (2006). "Novel cellulose fibre reinforced thermoplastic materials," *Cellulose* 13(3), 271-280.
Goetz, L., Mathew, A., Oksman, K., Gatenholm, P., and Ragauskas, A. J. (2009). "A novel nanocomposite film prepared from crosslinked cellulosic whiskers," *Carbohydrate Polymers* 75(1), 85-89.
Herrick, F. W., Casebier, R. L., Hamilton, J. K., and Sandberg, K. R. (1983). "Microfibrillated cellulose: Morphology and accessibility," *Journal of Applied Polymer Science* 37(9), 797-813.
Ho, C., and Zydney, A. L. (1999). "Effect of membrane morphology on the initial rate of protein fouling during microfiltration," *Journal of Membrane Science* 155(2), 261-275.
Hubbe, M. A., Rojas, O. J., Lucia, L. A., and Sain, M. (2008). "Cellulosic nanocomposites: A review," *BioResources* 3(3), 929-980.
Khulbe, K. C., Feng, C. Y., Matsuura, T., Mosqueada-Jimenaez, D. C., Rafat, M., Kingston, D., Narbaitz, R. M., and Khayet, M. (2007). "Characterization of surface-modified hollow fiber polyethersulfone membranes prepared at different air gaps," *Journal of Applied Polymer Science* 104(2), 710-721.
Khulbe, K. C., Matsuura, T., Singh, S., Lamarche, G., and Noh, S. H. (2000). "Study on fouling of ultrafiltration membrane by electron spin resonance," *Journal of Membrane Science* 167(2), 263-273.
Kim, I. C., Choi, J. G., and Tak, T. M. (1999). "Sulfonated polyethersulfone by heterogeneous method and its membrane performances," *Journal of Applied Polymer Science* 74(8), 2046-2055.
Lee, S. Y., Mohan, D. J., Kang, I. A., Doh, G. H., Lee, S., and Han, S. O. (2009). "Nanocellulose reinforced PVA composite films: Effects of acid treatment and filler loading," *Fibers and Polymers* 10(1), 77-82.
Li, J., Xu, Z., and Yang, H. (2008). "Microporous polyethersulfone membranes prepared under the combined precipitation conditions with non-solvent additives," *Polymers for Advanced Technologies* 19(4), 251-257.
Li, R., Fei, J., Cai, Y., Li, Y., Feng, J., and Yao, J. (2009). "Cellulose whiskers extracted from mulberry: A novel biomass production," *Carbohydrate Polymers* 76(1), 94-99.
Lindau, J., and Jönsson, A.-S. (1999). "Adsorptive fouling of modified and unmodified commercial polymeric ultrafiltration membranes," *Journal of Membrane Science* 160(1), 65-76.
Lu, J., Askeland, P., and Drzal, L. T. (2008). "Surface modification of microfibrillated cellulose for epoxy composite applications," *Polymer* 49(5), 1285-1296.
Madaeni, S. S., and Rahimpour, A. (2005). "Effect of type of solvent and non-solvents on morphology and performance of polysulfone and polyethersulfone ultrafiltration

membranes for milk concentration," *Polymers for Advanced Technologies* 16(10), 717-724.

Morán, J., Alvarez, V., Cyras, V., and Vázquez, A. (2008). "Extraction of cellulose and preparation of nanocellulose from sisal fibers," *Cellulose* 15(1), 149-159.

Nishino, T., Takano, K., and Nakamae, K. (1995). "Elastic modulus of the crystalline regions of cellulose polymorphs," *Journal of Polymer Science Part B: Polymer Physics* 33(11), 1647-1651.

Oksman, K., Mathew, A. P., Bondeson, D., and Kvien, I. (2006). "Manufacturing process of cellulose whiskers/polylactic acid nanocomposites," *Composites Science and Technology* 66(1), 2776-2784.

Qu, P., Gao, Y., Wu, G. F., and Zhang, L. P. (2010). "Nanocomposites of poly(lactic acid) reinforced with cellulose nanofibrils," *BioResources* 5(3), 1811-1823.

Rahimpour, A., Madaeni, S., and Mansourpanah, Y. (2007). "The effect of anionic, non-ionic and cationic surfactants on morphology and performance of polyethersulfone ultrafiltration membranes for milk concentration," *Journal of Membrane Science* 296(1-2), 110-121.

Yu, L., Shen, H., and Xu, Z. (2009). "PVDF-TiO_2 composite hollow fiber ultrafiltration membranes prepared by TiO_2 sol-gel method and blending method," *Journal of Applied Polymer Science* 113(3), 1763-1772.

Zhang, L., Chen, G., Tang, H., Cheng, Q., and Wang, S. (2009). "Preparation and characterization of composite membranes of polysulfone and microcrystalline cellulose," *Journal of Applied Polymer Science* 112(1), 550-556.

Zuluaga, R., Putaux, J. L., Cruz, J., Vlez, J., Mondragon, I., and Gan, P. (2009). "Cellulose microfibrils from banana rachis: Effect of alkaline treatments on structural and morphological features," *Carbohydrate Polymers* 76(1), 51-59.

Article submitted: July 17, 2010; Peer review completed: August 24, 2010; Revised version received and accepted: September 12, 2010; Published: September 14, 2010.